

# Histone deacetylase 6 delays motor neuron degeneration by ameliorating the autophagic flux defect in a transgenic mouse model of amyotrophic lateral sclerosis

Sheng Chen<sup>1</sup>, Xiao-Jie Zhang<sup>1</sup>, Li-Xi Li<sup>1</sup>, Yin Wang<sup>2</sup>, Ru-Jia Zhong<sup>2</sup>, Weidong Le<sup>1,2</sup>

<sup>1</sup>Department of Neurology, Ruijin Hospital, Shanghai Jiaotong University School of Medicine, Shanghai 200025, China

<sup>2</sup>Center for Translational Research on Neurological Diseases, First Affiliated Hospital of Dalian Medical University, Dalian 116011, China

Corresponding author: Weidong Le. E-mail: [wdle@sibs.ac.cn](mailto:wdle@sibs.ac.cn)

© Shanghai Institutes for Biological Sciences, CAS and Springer-Verlag Berlin Heidelberg 2015

## ABSTRACT

Amyotrophic lateral sclerosis (ALS) is a fatal neurodegenerative disorder characterized by the selective loss of motor neurons. Abnormal protein aggregation and impaired protein degradation are believed to contribute to the pathogenesis of this disease. Our previous studies showed that an autophagic flux defect is involved in motor neuron degeneration in the SOD1<sup>G93A</sup> mouse model of ALS. Histone deacetylase 6 (HDAC6) is a class II deacetylase that promotes autophagy by inducing the fusion of autophagosomes to lysosomes. In the present study, we showed that HDAC6 expression was decreased at the onset of disease and became extremely low at the late stage in ALS mice. Using lentivirus-HDAC6 gene injection, we found that HDAC6 overexpression prolonged the lifespan and delayed the motor neuron degeneration in ALS mice. Moreover, HDAC6 induced the formation of autolysosomes and accelerated the degradation of SOD1 protein aggregates in the motor neurons of ALS mice. Collectively, our results indicate that HDAC6 has neuroprotective effects in an animal model of ALS by improving the autophagic flux in motor neurons, and autophagosome-lysosome fusion might be a therapeutic target for ALS.

**Keywords:** motor neuron disease; motor neuron;

neurodegenerative disease; amyotrophic lateral sclerosis; autophagy; histone deacetylase 6

## INTRODUCTION

Amyotrophic lateral sclerosis (ALS) is a fatal, adult-onset neurodegenerative disease<sup>[1-3]</sup>. Pathologically, it is characterized by progressive, selective motor neuron loss in the brain and spinal cord<sup>[2,3]</sup>. Mutations in copper/zinc superoxide dismutase (SOD1) account for ~20% of familial cases of ALS<sup>[3, 4]</sup>. In this study, mice overexpressing the G93A mutation of SOD1 were used to model ALS. The underlying pathogenic mechanisms, although still largely unknown, probably involve the aggregation of misfolded proteins<sup>[5, 6]</sup>.

There are two main systems for cytoplasmic protein degradation: the ubiquitin-proteasome system and the autophagy-lysosome system<sup>[7]</sup>. Autophagy is a lysosome-based bulk-degradation pathway to clear misfolded proteins and toxic aggregates. Dysfunction of the autophagy-lysosome system may contribute to neuronal degeneration in several neurodegenerative diseases<sup>[6,8,9]</sup>. Our previous study and those of others have shown the accumulation of autophagic vacuoles in the spinal cord of SOD1<sup>G93A</sup> mice and ALS patients, suggesting a role of autophagy in the pathogenesis of ALS<sup>[5, 10]</sup>. We further reported that targeting autophagy with rapamycin, a classic autophagy activator, significantly exacerbates motor neuron loss and fails to

remove the abnormal mutant SOD1 aggregates, raising the possibility of autophagic flux defects in SOD1<sup>G93A</sup> mice<sup>[11]</sup>. Our latest study demonstrated that trehalose, an mTOR (mammalian target of rapamycin)-independent autophagy inducer, is able to decrease SOD1 and ubiquitinated protein accumulation as well as improve autophagic flux in the motor neurons of ALS mice, suggesting that the strategy of improving autophagic flux may have potential in ALS treatment<sup>[12]</sup>.

Histone deacetylase 6 (HDAC6) is a unique class II deacetylase containing a ubiquitin-binding domain; it copes with excessive levels of misfolded proteins by recruiting them to dynein motors for transport to aggresomes<sup>[13, 14]</sup>. Furthermore, HDAC6 is a central component of the aggresome that promotes autophagy by inducing the fusion of autophagosomes to lysosomes and regulates the protective response to the formation of cytotoxic protein aggregates<sup>[15, 16]</sup>. Accumulating evidence has shown that HDAC6-induced autophagy rescues neurons from degeneration in animal models of Huntington's disease, Alzheimer's disease, and Parkinson's disease<sup>[17, 18]</sup>. However, little is known about the effects of HDAC6 on ALS.

In this study, we investigated the effects of HDAC6 on motor neuron degeneration in a mouse model of ALS through intracerebroventricular injection of lentivirus-HDAC6 into SOD1<sup>G93A</sup> transgenic mice, and explored the underlying mechanisms.

## MATERIALS AND METHODS

### Mice and Treatments

Transgenic SOD1<sup>G93A</sup> mice expressing mutant human SOD1 with a Gly93Ala substitution (B6SJL-Tg-SOD1G93A-1Gur) were originally obtained from Jackson Laboratories (002726, Sacramento, CA). All mice were housed under constant temperature and controlled light. Animal use was approved by the Ethics Committee of Shanghai Jiaotong University School of Medicine and all procedures in our experiments were conducted in accordance with the guidelines of National Institute of Health for animal care.

The genotypes of the transgenic mice were identified by PCR as in our previous reports<sup>[11, 12]</sup>. Male SOD1<sup>G93A</sup> mice were randomly divided into 2 groups (Tg-Control and

Tg-HDAC6, 18 mice in each). Those in the Tg-HDAC6 group were injected with HDAC6 lentivirus and those in the Tg-Control group were injected with the same volume of control lentivirus. Meanwhile, 36 age-matched wild-type (WT) littermates were divided into WT-Control and WT-HDAC6 groups. All the mice were weighed every four days from 94 to 146 days after birth. The mean body weight for each group at each time point was recorded.

### Plasmids and Clones

Full-length human *HDAC6* (NM\_006044) was cloned by PCR. The primers for *HDAC6* target sequences were as follows: forward 5'-CTCAAGCTTCGAATTCGCCACCATG-ACCTCAACCGGCCAG-3'; reverse 5'-CCTTGTAGTCGGA-TCCGTGTGGGTGGGGCATATC-3'. Full-length cDNA of HDAC6 was cloned into the pLVX-3Flag-puro lentiviral vector. All constructs were verified by sequencing. The pLVX-3Flag-puro lentiviral vector itself was used as the control. The lentiviral and help vectors (SBO Medical Biotech, Shanghai, China) were transfected into 293FT cells for viral packaging.

### Intracerebroventricular Injection of Lentiviruses

Large-scale lentivirus production and purification were as described previously<sup>[19]</sup>. In brief, 293FT cells were infected with each lentiviral vector and help vector for viral packaging. After harvesting and shaking, the PEG-800-NaCl system (Sigma-Aldrich, St. Louis, MO) was used to purify and concentrate the lentivirus. The titers of the virus preparation were  $6-8 \times 10^8$  vector genomes per milliliter. The mice were anesthetized with chloral hydrate and 8  $\mu$ L HDAC6 lentivirus or control lentivirus was injected into the right cerebral ventricle (AP: -0.22 mm, ML: -1.0 mm, DV: -2.35 mm) at 1  $\mu$ L/min.

### Behavioral Tests

#### Assessment of Disease Onset (Rotarod Test)

SOD1<sup>G93A</sup> transgenic mice showing disease onset were used for lentivirus injection. Rotarod performance was measured every day in these mice starting at 72 days of age. The date of disease onset was defined as when a mouse could not stay on the rotating rod for 5 min<sup>[20]</sup>. Based on rotarod performance, lentivirus injection was started at 95 days of age.

### Assessment of Lifespan

For lifespan analysis, the date of “death” was defined as the day when a mouse could not right itself within 30 s after being placed on its back<sup>[21]</sup>. All the mice were tested every day and the date of “death” was recorded.

### Immunofluorescence Staining

Each mouse was anesthetized, perfused with PBS, and fixed with 4% paraformaldehyde. The spinal cord was removed and postfixed in 4% paraformaldehyde at 4°C overnight, then cryoprotected in 15% sucrose for 24 h and 30% sucrose for another 24 h. The spinal cord was cut into 10- $\mu$ m-thick sections on a sliding microtome (Leica 3050s, Nussloch, Germany). Slides were incubated at 4°C overnight with primary antibodies against LC3B (1:200; Cell Signaling, Danvers, MA), SOD1 (1:200; Abcam, HK), or p62 (1:100; BD Transduction Laboratories, Waltham, MA). After washing with PBS, the slides were incubated with secondary antibody Cy2 or Cy3 (Jackson ImmunoResearch, West Grove, PA), and then visualized at 600 $\times$  magnification under a fluorescence microscope (Nikon Eclipse 80i, Tokyo, Japan). Motor neurons were identified in the anterior horn, with cell bodies >20  $\mu$ m. Slides incubated with secondary antibody Cy2 or Cy3 alone were used as a negative control. In each animal, the images of 20 randomly-selected motor neurons were captured and the number of LC3- or p62-positive puncta in each motor neuron was counted by a researcher who was blinded to the experimental design.

### Analysis of Motor Neuron Survival

The fixed L4–5 segments were cut into 10- $\mu$ m sections, which were Nissl stained with 1% cresyl violet (Sigma-Aldrich). Every fifth section was selected from the total 250 serial sections from each mouse. The 50 sections from each mouse were photographed under a microscope (Olympus IX81, Tokyo, Japan) and the anterior horns on both sides were examined by a technician who was blinded to the experimental design. The number of motor neurons was counted as described previously<sup>[21, 22]</sup>.

### Immunoblotting

For immunoblotting, 40 mg of lysed protein was separated on SDS-PAGE gel and transferred to PVDF membrane. Membranes were incubated with the primary antibodies

against HDAC6 (1:1 000, Cell Signaling), LC3B (1:500, Cell Signaling), p62 (1:500, MBL, Nagoya, Japan), or Flag (1:1 000, Cell Signaling). After incubation overnight, secondary antibodies were applied and protein bands were visualized using chemiluminescent horseradish peroxidase substrate (ECL, Pierce, Waltham, MA) and quantified with an image analyzer (Image Lab 4.2, Bio-Rad, Hercules, CA).  $\beta$ -actin (1:6 000; Sigma-Aldrich) was used as an internal control.

### Quantitative Real-time PCR

Total RNA was extracted from homogenized spinal cord samples (from 60-, 90-, and 120-day-old Tg and WT mice) with TRIzol reagent (Invitrogen, Carlsbad, CA). Two milligrams of total RNA were used for cDNA synthesis using the ReverTra Ace qPCR RT Kit (Toyobo, Osaka, Japan). Real-time PCR was performed using the SYBR premix Ex Taq TM II kit (Takara, Shiga, Japan) and analyzed using a real-time PCR System (ABI7500). The sequences of primers were as follows: HDAC6, forward 5'-ATAGCAGCACTACCTGGGAAAG-3' and reverse 5'-TTAGGGAAGTTTTTCAGGAGCAG-3'; GAPDH, forward 5'-CCAATGTGTCCGTCGTGGATCT-3' and reverse 5'-GTTGAAGTCGCAGGAGACAACC-3'.

### Electron Microscopy

Electron microscopy (EM) was performed as reported previously<sup>[11, 12]</sup>. In brief, L4–5 segments were fixed in 2.5% glutaraldehyde and cut into 50- $\mu$ m sections. Then, the sections were postfixed in 1% OsO<sub>4</sub>, dehydrated, embedded, and further cut into 70-nm sections. The ultra-thin sections were stained with uranyl acetate and evaluated with a CM-120 EM (Philips, Eindhoven, The Netherlands). EM images were captured at a final magnification of 10 000 $\times$ . Autolysosome was defined as single-membrane structures containing cytoplasmic material and/or organelles<sup>[23]</sup>.

### Statistical Analysis

Kaplan-Meier analysis (SPSS 17.0) was performed for lifespan data and the data were analyzed using the log-rank test, generating a  $\chi^2$  value to test for significance. Data of Flag-HDAC6 expression were analyzed using one-way ANOVA followed by Tukey's *post hoc* test. Other data were analyzed with two-way ANOVA (Prism 5, GraphPad

Software, La Jolla, CA). All values are presented as mean  $\pm$  SEM.  $P < 0.05$  was defined as statistically significant.

## RESULTS

### HDAC6 Expression in the Spinal Cord of SOD1<sup>G93A</sup> and WT Mice

Immunoblotting revealed that the level of HDAC6 markedly decreased in an age-dependent manner in the spinal cord of SOD1<sup>G93A</sup> mice. This started at 90 days of age and became more evident at 120 days, while there were no significant differences between the levels in 60-, 90-, and 120-day-old WT mice (Fig. 1A). Analysis showed that the level of HDAC6 protein in the spinal cord of SOD1<sup>G93A</sup> mice fell to 70.44% at 90 days and to 40.88% at 120 days of that in age-matched WT mice (Fig. 1B). In addition, there was a significant reduction in HDAC6 mRNA levels in the spinal cord of 90- and 120-day-old SOD1<sup>G93A</sup> mice compared with

age-matched WT mice (Fig. 1C). These results showed that HDAC6 expression decreases in SOD1<sup>G93A</sup> mice at both the transcriptional and translational levels in an age-dependent manner.

To further investigate the expression of lentivirus-HDAC6 in the mouse spinal cord, immunoblotting was used to assess the levels of Flag 2, 4, 6, and 8 weeks after HDAC6 lentivirus injection. The Flag-HDAC6 expression in the spinal cord increased from 2 weeks to 4 weeks after HDAC6 lentivirus injection, then decreased with time (Fig. 1D, E).

### HDAC6 Overexpression Prolonged the Lifespan of SOD1<sup>G93A</sup> Mice

We injected the HDAC6 lentivirus into SOD1<sup>G93A</sup> mice at disease onset based on rotarod performance, which was usually at the age of 95 days<sup>[11, 12]</sup>. We found that Tg-HDAC6 mice had a 17-day extension in lifespan compared with Tg-Control mice ( $140.00 \pm 4.33$  vs  $123.00 \pm 2.60$ ,

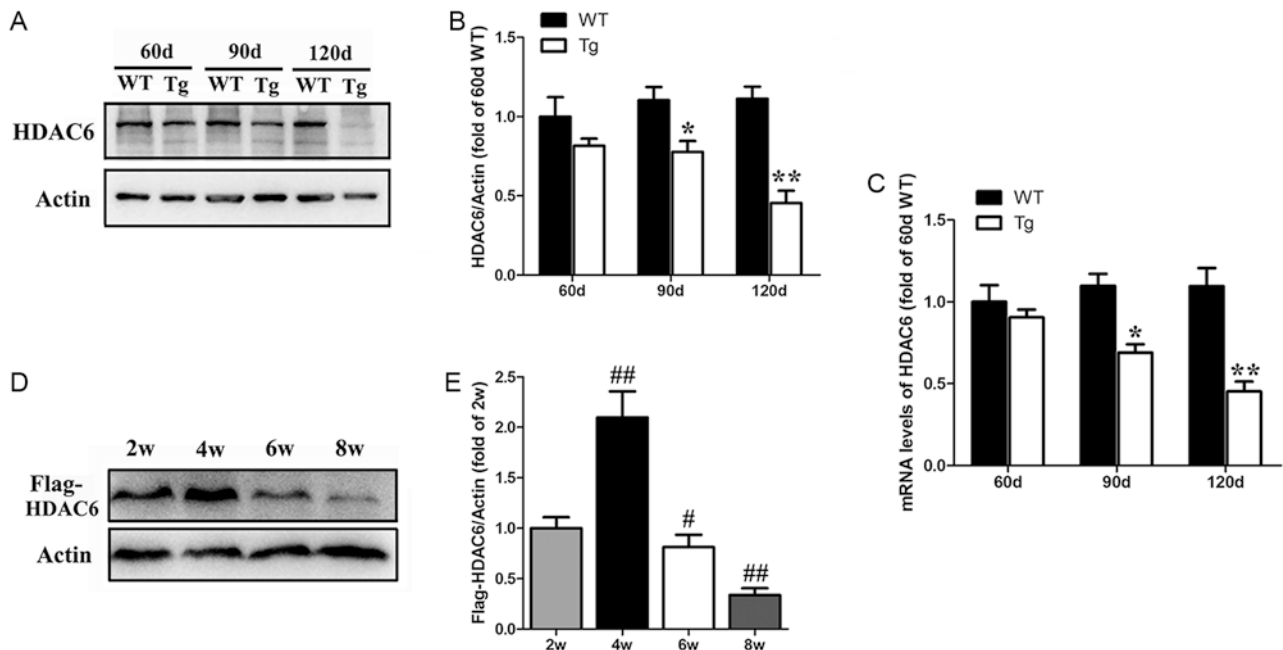


**Fig. 1.** HDAC6 expression in wild-type (WT) and transgenic (Tg) mice. (A) Immunoblots of HDAC6 expression in the spinal cord of 60-, 90-, 120-day-old G93A Tg and age-matched WT mice. (B) Analysis of HDAC6/actin in WT and Tg mice. (C) HDAC6 mRNA expression in the spinal cord as assessed by real-time PCR in WT and Tg mice. (D) Immunoblots of Flag-HDAC6 expression in the spinal cord of Tg mice at 2, 4, 6, and 8 weeks after lentivirus injection. (E) Analysis of Flag-HDAC6/actin at 2, 4, 6, and 8 weeks after lentivirus injection.  $n = 3$  mice/group. Data in B and C were analyzed using two-way ANOVA with repeated measures. Data in E were analyzed using one-way ANOVA followed by Tukey's *post hoc* test. All values are presented as mean  $\pm$  SEM. \* $P < 0.05$  compared with 90-day-old WT mice; \*\* $P < 0.01$  compared with 120-day-old WT mice; ## $P < 0.05$ , ### $P < 0.01$  compared with 2-week group.



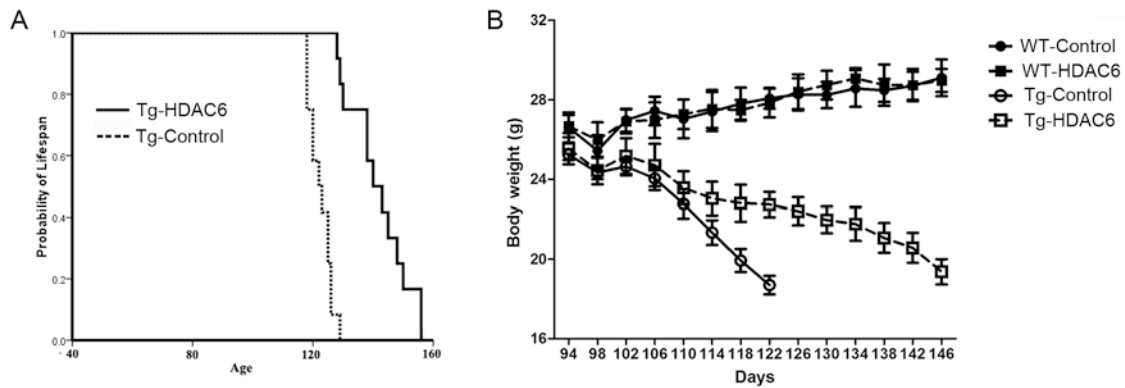


Fig. 2. Effects of HDAC6 overexpression on lifespan and body weight in WT and Tg mice. (A) Kaplan-Meier survival analysis showing the probability of survival in Tg-Control (dotted line) and Tg-HDAC6 mice (solid line). (B) Body weight curves in the 4 groups.  $n = 10/\text{group}$ .

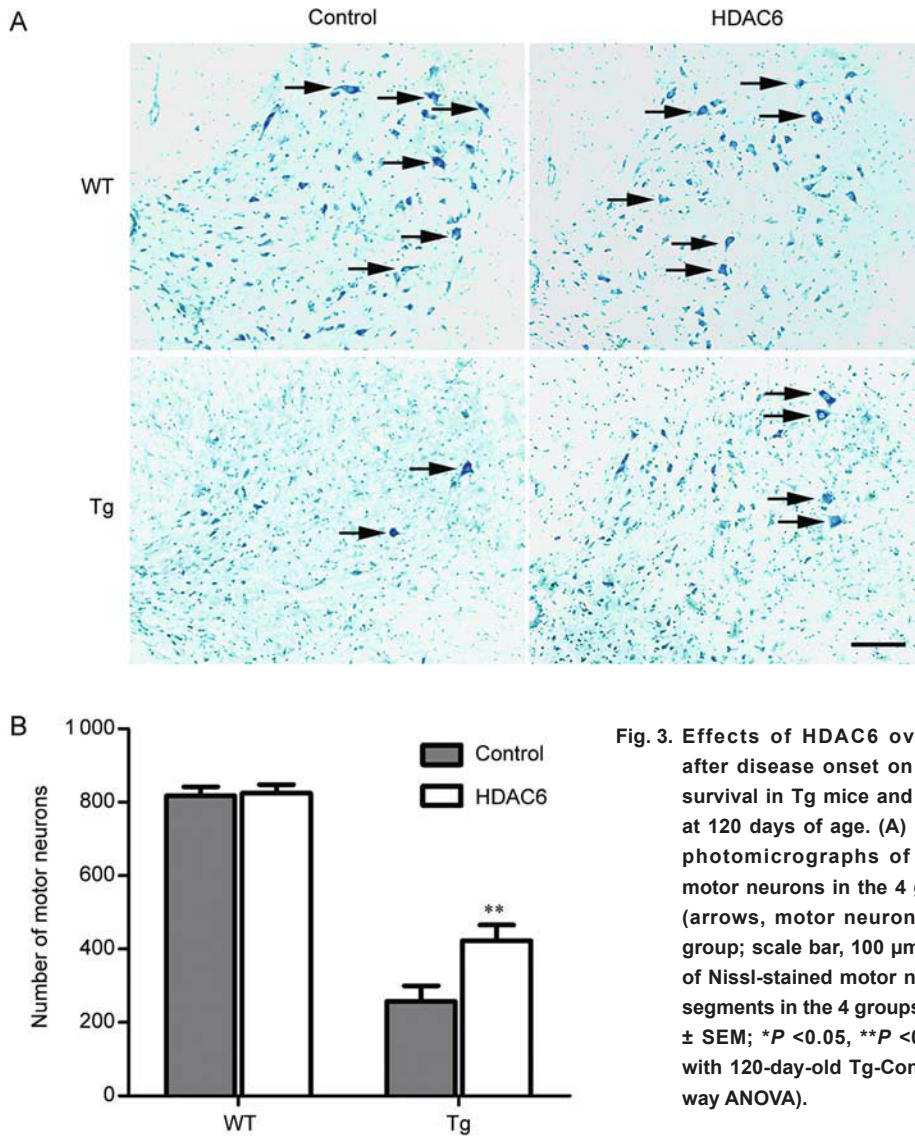


Fig. 3. Effects of HDAC6 overexpression after disease onset on motor neuron survival in Tg mice and in WT siblings at 120 days of age. (A) Representative photomicrographs of Nissl-stained motor neurons in the 4 groups of mice (arrows, motor neurons;  $n = 3$  mice/group; scale bar, 100  $\mu\text{m}$ ). (B) Numbers of Nissl-stained motor neurons in L4-5 segments in the 4 groups of mice (mean  $\pm$  SEM;  $*P < 0.05$ ,  $**P < 0.01$  compared with 120-day-old Tg-Control mice; two-way ANOVA).

$\chi^2 = 23.76$ ,  $P < 0.01$ ) (Fig. 2A). Moreover, Tg-HDAC6 mice exhibited a significant reduction in body weight loss compared with age-matched Tg-Control mice (Fig. 2B). However, there was no difference in body weight between WT-Control and WT-HDAC6 mice.

#### HDAC6 Overexpression Protected Motor Neurons in SOD1<sup>G93A</sup> Mice

Nissl staining showed a significant loss of motor neurons in the L4–5 segments of 120-day-old SOD1<sup>G93A</sup> mice compared with WT mice (Fig. 3A, B). In addition, the number of motor neurons in the Tg-HDAC6 mice was markedly higher than that in Tg-Control mice ( $423.0 \pm 31.25$  vs  $257.5 \pm 21.32$ ,  $P < 0.01$ ; Fig. 3B). Motor neuron survival did not differ between WT-Control and WT-HDAC6 mice ( $817.30 \pm 36.03$  vs  $824.80 \pm 42.03$ ,  $P > 0.05$ ) (Fig. 3A, B).

#### HDAC6 Overexpression Reduced the Aggregation of LC3-Positive Puncta in Motor Neurons of SOD1<sup>G93A</sup> Mice

Previous studies have reported that HDAC6 plays an important role in the process of autophagy<sup>[15]</sup>. To determine the effect of HDAC6 in this process, we used

immunoblotting to determine the LC3-II turnover in the spinal cord of 120-day-old SOD1<sup>G93A</sup> mice, and found that HDAC6 overexpression decreased the elevated LC3-II level by ~30.2% (Fig. 4A, B). Immunofluorescence staining further revealed a decrease of LC3-positive puncta in the motor neurons of Tg-HDAC6 mice compared with the Tg-Control mice (Fig. 4C, D). These results showed that HDAC6 overexpression at disease onset reduces the premature autophagy in the motor neurons of SOD1<sup>G93A</sup> mice.

#### HDAC6 Overexpression Improved Autophagic Flux in SOD1<sup>G93A</sup> Mice

To further investigate the effects of HDAC6 overexpression on autophagic flux, we determined the protein level of p62, a biomarker of autophagic flux<sup>[24]</sup>, in the spinal cord of SOD1<sup>G93A</sup> mice. Immunoblotting showed an abnormally high level of p62 protein in the spinal cord of SOD1<sup>G93A</sup> mice compared with WT mice; HDAC6 overexpression reduced the elevated p62 level in the SOD1<sup>G93A</sup> mice (Fig. 5A) by 34.08% (Fig. 5B). Further, p62 immunostaining showed a significant decrease of p62-positive aggregation in the motor neurons of Tg-HDAC6 mice compared with

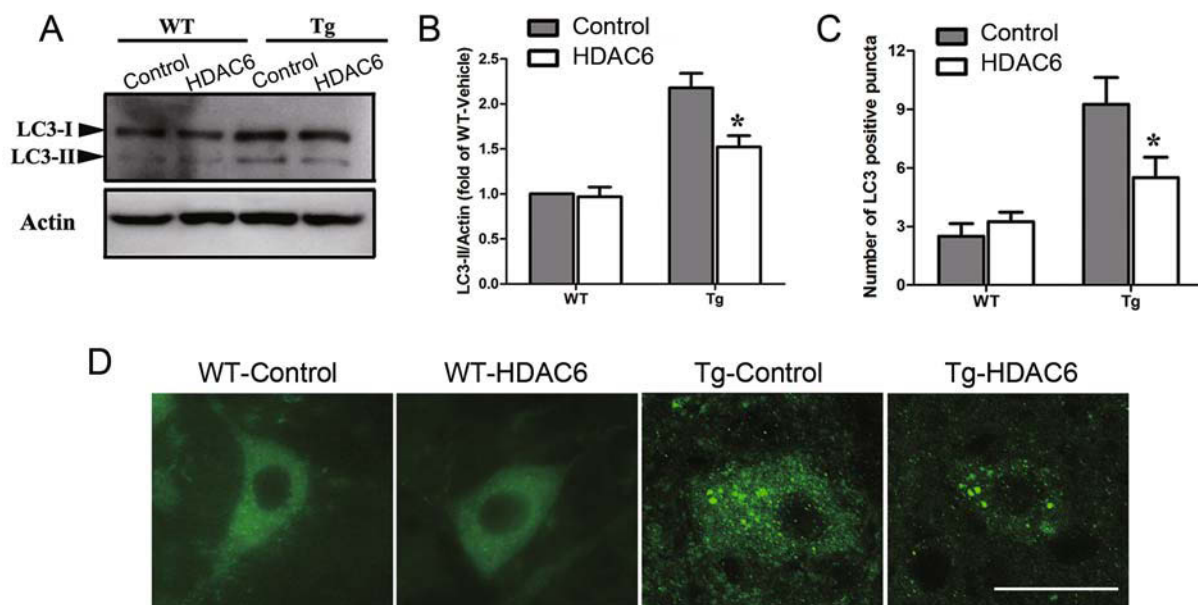


**Fig. 4.** Effects of HDAC6 overexpression on the number of autophagosomes in G93A Tg mice. (A) Immunoblots of LC3-II expression in the spinal cord of 120-day-old WT and Tg mice. (B, C) Analysis of LC3-II/actin in 120-day-old WT and Tg mice (B) and numbers of LC3-II-positive puncta (C) in the 4 groups of mice (mean  $\pm$  SEM.; \* $P < 0.05$  compared with 120-day-old Tg-Control mice; two-way ANOVA). (D) Immunostaining of LC3 in motor neurons of the 4 groups of mice (scale bar, 20  $\mu$ m).

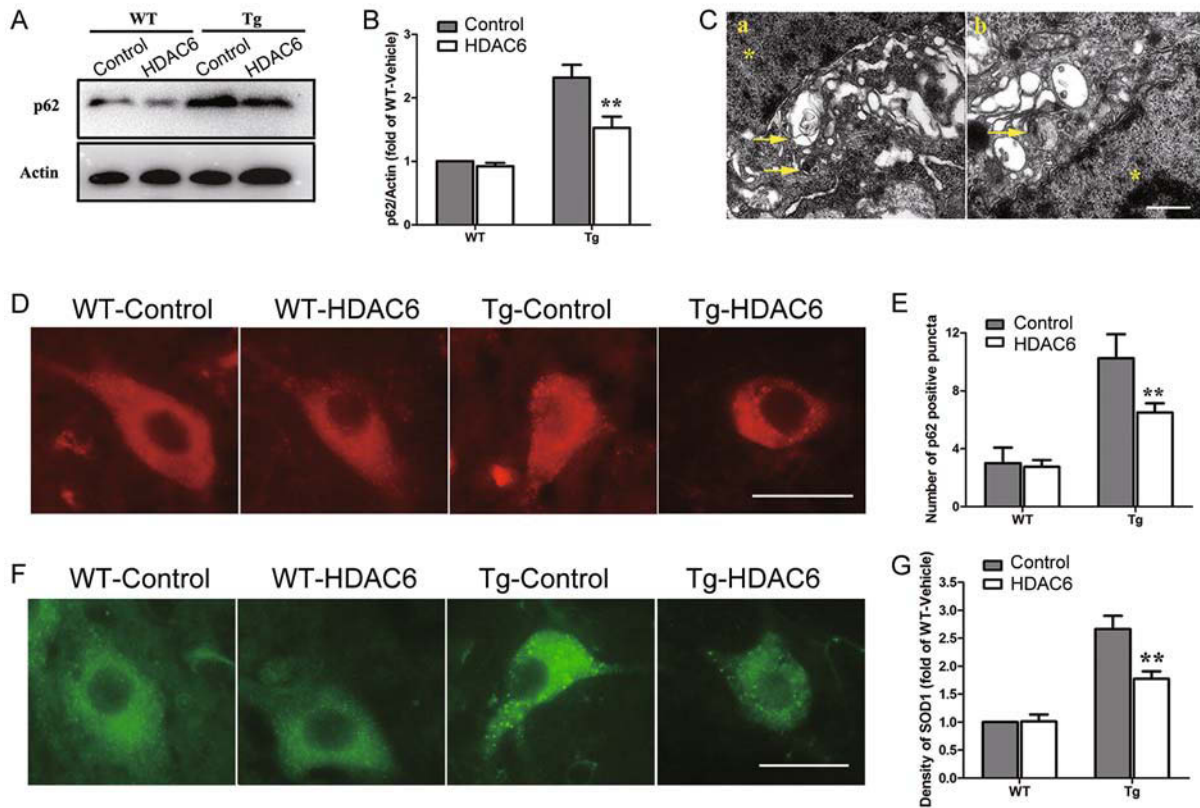


**Fig. 5.** Effects of HDAC6 overexpression on autophagic flux and SOD1 protein degradation in G93A Tg mice. (A) Immunoblots of p62 expression in the spinal cord of 120-day-old WT and Tg mice. (B) Analysis of p62/actin in 120-day-old WT and Tg mice. (C) Representative electron microscopic images of autolysosomes in the spinal motor neurons of 120-day-old Tg-HDAC6 mice (arrows, autolysosomes; \*nucleus; scale bar, 0.5  $\mu$ m). (D-G) Immunostaining of p62 (D) and SOD1 (F) in motor neurons from the 4 groups of mice (scale bars, 20  $\mu$ m), and analysis of p62-positive puncta (E) and SOD1 density (G) in the motor neurons of 120-day-old WT and Tg mice (mean  $\pm$  SEM; \*\* $P$  < 0.01 compared with 120-day-old Tg-Control mice; two-way ANOVA).

Tg-Control mice ( $6.50 \pm 1.71$  vs  $10.25 \pm 2.95$ ) (Fig. 5D, E). Moreover, EM examination further showed single-membrane structures of autolysosomes in the motor neurons of Tg-HDAC6 mice (Fig. 5C), providing more evidence for HDAC6-mediated autophagic protein degradation in SOD1<sup>G93A</sup> mice.

We further found a significant decrease in SOD1 aggregates in the Tg-HDAC6 mice compared with the Tg-Control mice (Fig. 5F). Analysis showed that the density of SOD1 immunostaining in the motor neurons of Tg-HDAC6 mice was reduced to 66.6% of that in Tg-Control mice (Fig. 5G).

## DISCUSSION

In this study, we first reported that the level of HDAC6

expression in the spinal cord of the SOD1<sup>G93A</sup> mouse model of ALS decreased, starting at disease onset, and became extremely low in later stages. Furthermore, HDAC6 overexpression at disease onset prolonged the lifespan by delaying motor neuron degeneration in the ALS model. Moreover, the neuroprotective action of HDAC6 might be related to its effect on autophagic flux and then the clearance of abnormal protein aggregates in the motor neurons of SOD1<sup>G93A</sup> mice.

According to previous reports, HDAC6 is highly conserved and the structure and function of mouse HDAC6 are similar to its human ortholog<sup>[25, 26]</sup>. The double catalytic domain, a ubiquitin-binding domain, and a nuclear export-signal domain are functionally conserved in mouse and human HDAC6, mediating the same deacetylase,

ubiquitin protein-binding, and nuclear protein export activities<sup>[27]</sup>. It has been documented that the ubiquitin-binding domain plays an important role in HDAC6-mediated autophagosome maturation and autophagosome-lysosome fusion<sup>[14, 15]</sup>. In this study, human HDAC6 was selected for overexpression, as it could provide evidence relevant to the clinical treatment of ALS.

Accumulating evidence has suggested that autophagic flux impairment plays a critical role in ALS<sup>[28, 29]</sup>. Our previous studies showed that the mTOR-dependent autophagic inducer rapamycin accelerates motor neuron loss and aggravates autophagic flux dysfunction in the SOD1<sup>G93A</sup> mouse model of ALS<sup>[11]</sup>. Our latest report provided strong evidence for an autophagic flux defect, especially impairment in the fusion of autophagosomes and lysosomes in the ALS model<sup>[12]</sup>. In the present study, we found that HDAC6 overexpression after disease onset reduced p62 and SOD1 aggregation, which was accompanied by decreased LC3-positive aggregates in the motor neurons of SOD1<sup>G93A</sup> mice. Furthermore, EM analysis showed the formation of autolysosomes in the motor neurons of Tg-HDAC6 mice. Otherwise, a previous study demonstrated that an autophagic protein marker is specifically increased in the spinal motor neurons of SOD1<sup>G93A</sup> mice, and not in microglia or astrocytes<sup>[11]</sup>. In the present study, we further found that the alterations of LC3-II and p62 puncta were mainly in the motor neurons after HDAC6 overexpression in SOD1<sup>G93A</sup> mice. These results suggested that HDAC6 improves autophagic flux by inducing the formation of autolysosomes in the motor neurons of ALS mice even at late stages of the disease.

It has been reported that microtubule-based vesicle trafficking, especially the fusion of autophagosomes and lysosomes, is critical for the autophagy process<sup>[30]</sup>. And impairment of dynein-mediated trafficking might be associated with the autophagosome-lysosome fusion defect<sup>[31]</sup>. Mutant SOD1 alters the cellular localization of dynein and inhibits the dynein-mediated trafficking in neurons, which might affect the microtubule-based autophagic fusion step in ALS<sup>[32]</sup>. HDAC6 acts as a multivalent adapter to bind both ubiquitinated proteins and dynein motors, recruiting misfolded protein cargos to the autophagosomes along the microtubules<sup>[14]</sup>. It is worth pointing out that HDAC6 stimulates the fusion of autophagosomes to lysosomes and substrate degradation

in neurons<sup>[15]</sup>. Several lines of evidence have documented that HDAC6 deficiency leads to autophagosome maturation failure, protein aggregation, and neurodegeneration<sup>[15, 33]</sup>. On the other hand, expression of HDAC6 at the normal level is sufficient to rescue neurodegeneration in an autophagy-dependent manner<sup>[17]</sup>. In our study, we found that overexpressing HDAC6 in Tg-HDAC6 mice significantly improved the autophagic flux and enhanced the clearance of protein aggregation in motor neurons, further supporting a role of HDAC6 in autophagy-dependent protein degradation in ALS.

Although recent studies have indicated that the induction of HDAC6 can be neuroprotective by removing protein aggregates in neurodegenerative diseases, the therapeutic strategy of targeting HDAC6 is still controversial<sup>[33, 34]</sup>. Specific inhibitors of HDAC6 or genetic knock-down of HDAC6 has shown neuroprotective effects by increasing the acetylation levels of  $\alpha$ -tubulin to improve axonal transport in neurons<sup>[35, 36]</sup>. It is not known whether inhibiting or deleting HDAC6 affects the expression of mutant SOD1<sup>G93A</sup>. The variable results may be due to the different functions of HDAC6 at different stages of the disease<sup>[37, 38]</sup>. It is likely that HDAC6 inhibition at the early stage is beneficial for ALS by restoring axonal transport, while HDAC6 is required to maintain autophagosome-lysosome fusion at the later stages of ALS when protein aggregation is dominant in the motor neurons of SOD1<sup>G93A</sup> mice. However, more studies are required to explore the detailed mechanisms of HDAC6 activity at different stages of ALS and to investigate the mechanisms underlying the age-dependent decrease of the HDAC6 level in ALS.

In summary, we first report that the level of HDAC6 is significantly decreased at disease onset in the SOD1<sup>G93A</sup> mouse model of ALS. HDAC6 overexpression at disease onset prolonged the lifespan and delayed the motor neuron degeneration in ALS mice. Moreover, we found that HDAC6 induced the formation of autolysosomes and accelerated the degradation of SOD1 protein aggregates in the motor neurons of ALS mice. Collectively, these results indicate that HDAC6 is a potential target for ALS treatment.

#### ACKNOWLEDGEMENTS

This work was supported by grants from the National Natural Science Foundation of China (81200977), the Shanghai



Natural Science Foundation (14ZR1446400), Shanghai Rising-Star Program (15QA1403000), the PhD Innovation Fund of Shanghai Jiaotong University School of Medicine (BXJ 201218), and the PhD Tutor Fund of the Ministry of Education of China (20120073110077).

Received date: 2015-05-12; Accepted date: 2015-06-10

## REFERENCES

- [1] Andersen PM. Amyotrophic lateral sclerosis associated with mutations in the CuZn superoxide dismutase gene. *Curr Neurol Neurosci Rep* 2006, 6: 37–46.
- [2] Chen S, Sayana P, Zhang X, Le W. Genetics of amyotrophic lateral sclerosis: an update. *Mol Neurodegener* 2013, 8: 28.
- [3] Pasinelli P, Brown RH. Molecular biology of amyotrophic lateral sclerosis: insights from genetics. *Nat Rev Neurosci* 2006, 7: 10–23.
- [4] Kirby J, Halligan E, Baptista MJ, Allen S, Heath PR, *et al.* Mutant SOD1 alters the motor neuronal transcriptome: implications for familial ALS. *Brain* 2005, 128: 1686–1706.
- [5] Li L, Zhang X, Le W. Altered macroautophagy in the spinal cord of SOD1 mutant mice. *Autophagy* 2008, 4: 290–293.
- [6] Banerjee R, Beal MF, Thomas B. Autophagy in neurodegenerative disorders: pathogenic roles and therapeutic implications. *Trends Neurosci* 2010, 33: 541–549.
- [7] Goldberg AL. Protein degradation and protection against misfolded or damaged proteins. *Nature* 2003, 426: 895–899.
- [8] Cheung ZH, Ip NY. Autophagy deregulation in neurodegenerative diseases - recent advances and future perspectives. *J Neurochem* 2011, 118: 317–325.
- [9] Wong E, Cuervo AM. Autophagy gone awry in neurodegenerative diseases. *Nat Neurosci* 2010, 13: 805–811.
- [10] Sasaki S. Autophagy in spinal cord motor neurons in sporadic amyotrophic lateral sclerosis. *J Neuropathol Exp Neurol* 2011, 70: 349–359.
- [11] Zhang X, Li L, Chen S, Yang D, Wang Y, Zhang X, *et al.* Rapamycin treatment augments motor neuron degeneration in SOD1(G93A) mouse model of amyotrophic lateral sclerosis. *Autophagy* 2011, 7: 412–425.
- [12] Zhang X, Chen S, Song L, Tang Y, Shen Y, Jia L, *et al.* MTOR-independent, autophagic enhancer trehalose prolongs motor neuron survival and ameliorates the autophagic flux defect in a mouse model of amyotrophic lateral sclerosis. *Autophagy* 2014, 10: 588–602.
- [13] Boyault C, Sadoul K, Pabion M, Khochbin S. HDAC6, at the crossroads between cytoskeleton and cell signaling by acetylation and ubiquitination. *Oncogene* 2007, 26: 5468–5476.
- [14] Kawaguchi Y, Kovacs JJ, McLaurin A, Vance JM, Ito A, Yao TP. The deacetylase HDAC6 regulates aggresome formation and cell viability in response to misfolded protein stress. *Cell* 2003, 115: 727–738.
- [15] Lee JY, Koga H, Kawaguchi Y, Tang W, Wong E, Gao YS, *et al.* HDAC6 controls autophagosome maturation essential for ubiquitin-selective quality control autophagy. *EMBO J* 2010, 29: 969–980.
- [16] Boyault C, Zhang Y, Fritah S, Caron C, Gilquin B, *et al.* HDAC6 controls major cell response pathways to cytotoxic accumulation of protein aggregates. *Gene Dev* 2007, 21: 2172–2181.
- [17] Pandey UB, Nie Z, Batlevi Y, McCray BA, Ritson GP, Nedelsky NB, *et al.* HDAC6 rescues neurodegeneration and provides an essential link between autophagy and the UPS. *Nature* 2007, 447: 859–863.
- [18] Simoes-Pires C, Zwick V, Nurisso A, Schenker E, Carrupt PA, Cuendet M. HDAC6 as a target for neurodegenerative diseases: what make it different from other HDACs? *Mol Neurodegener* 2013, 29: 7.
- [19] Tang Y, Li T, Li J, Yang J, Liu H, Zhang XJ, *et al.* Jmjd3 is essential for the epigenetic modulation of microglia phenotypes in the immune pathogenesis of Parkinson's disease. *Cell Death Differ* 2014, 21:369–380.
- [20] Song L, Chen L, Zhang X, Li J, Le W. Resveratrol ameliorates motor neuron degeneration and improves survival in SOD1(G93A) mouse model of amyotrophic lateral sclerosis. *Biomed Res Int* 2014, 2014: 483501.
- [21] Zhang X, Chen S, Li L, Wang Q, Le W. Folic acid protects motor neurons against the increased homocysteine inflammation and apoptosis in SOD1G93A transgenic mice. *Neuropharmacology* 2008, 54: 1112–1119.
- [22] Manabe Y, Nagano I, Gazi MS, Murakami T, Shiote M, Shoji M, *et al.* Glial cell line-derived neurotrophic factor protein prevents motor neuron loss of transgenic model mice for amyotrophic lateral sclerosis. *Neurol Res* 2003, 25: 195–200.
- [23] Nixon RA, Wegiel J, Kumar A, Yu WH, Peterhoff C, Cataldo A, Cuervo AM. Extensive involvement of autophagy in Alzheimer disease: an immunoelectron microscopy study. *J Neuropathol Exp Neurol* 2005, 64: 113–122.
- [24] Klionsky DJ, Abdalla FC, Abeliovich H, Abraham RT, Acevedo-Arozena A, Adeli K, *et al.* Guidelines for the use and interpretation of assays for monitoring autophagy. *Autophagy* 2012, 8: 445–544.
- [25] Grozinger CM, Hassig CA, Schreiber SL. Three proteins define a class of human histone deacetylases related to yeast Hda1p. *Proc Natl Acad Sci U S A* 1999, 96: 4868–4873.
- [26] Verdell A, Khochbin S. Identification of a new family of higher eukaryotic histone deacetylases. Coordinate expression of differentiation-dependent chromatin modifiers. *J Biol Chem*

- 1999, 274: 2440–2445.
- [27] Boyault C, Sadoul K, Pabion M, Khochbin S. HDAC6, at the crossroads between cytoskeleton and cell signaling by acetylation and ubiquitination. *Oncogene* 2007, 26: 5468–5476
- [28] Chen S, Zhang X, Song L, Le W. Autophagy dysregulation in amyotrophic lateral sclerosis. *Brain Pathol* 2012, 22: 110–116.
- [29] Nassif M, Hetz C. Targeting autophagy in ALS: a complex mission. *Autophagy* 2011, 7: 450–453.
- [30] Laird FM, Farah MH, Ackerley S, Hoke A, Maragakis N, Rothstein JD, et al. Motor neuron disease occurring in a mutant dynactin mouse model is characterized by defects in vesicular trafficking. *J Neurosci* 2008, 28: 1997–2005.
- [31] Webb JL, Ravikumar B, Rubinsztein DC. Microtubule disruption inhibits autophagosome-lysosome fusion: implications for studying the roles of aggresomes in polyglutamine diseases. *Int J Biochem Cell Biol* 2004, 36: 2541–2550.
- [32] Zhang F, Ström AL, Fukada K, Lee S, Hayward LJ, Zhu H. Interaction between familial amyotrophic lateral sclerosis (ALS)-linked SOD1 mutants and the dynein complex. *J Biol Chem* 2007, 282: 16691–16699.
- [33] Du G, Jiao R. To prevent neurodegeneration: HDAC6 uses different strategies for different challenge. *Autophagy* 2011, 4: 139–142.
- [34] Zilberman Y, Ballestrem C, Carramusa L, Mazitschek R, Khochbin S, Bershadsky A. Regulation of microtubule dynamics by inhibition of the tubulin deacetylase HDAC6. *J Cell Sci* 2009, 122: 3531–3541.
- [35] Lazo-Gomez R, Ramirez-Jarquín UN, Tovar-Y-Romo LB, Tapia R. Histone deacetylases and their role in motor neuron degeneration. *Front Cell Neurosci* 2013, 7: 243.
- [36] Taes I, Timmers M, Hersmus N, Bento-Abreu A, Van Den B, Van Damme P, et al. Hdac6 deletion delays disease progression in the SOD1G93A mouse model of ALS. *Hum Mol Genet* 2013, 22: 1783–1790.
- [37] Marinkovic P, Reuter MS, Brill MS, Godinho L, Kerschensteiner M, Misgeld T. Axonal transport deficits and degeneration can evolve independently in mouse models of amyotrophic lateral sclerosis. *Proc Natl Acad Sci U S A* 2012, 109: 4296–4301.
- [38] Bilsland LG, Sahai E, Kelly G, Golding M, Greensmith L, Schiavo G. Deficits in axonal transport precede ALS symptoms *in vivo*. *Proc Natl Acad Sci U S A* 2010, 107: 20523–20528.